

APPLICATIONS OF LOCKIN-THERMOGRAPHY METHODS

D. Wu¹, J. Rantala², W. Karpen¹, G. Zenzinger³, B. Schönbach⁴, W. Rippel¹,
R. Steegmüller¹, L. Diener¹, G. Busse¹

¹Institut für Kunststoffprüfung und Kunststoffkunde (IKP)
University of Stuttgart
Pfaffenwaldring 32
D-70569 Stuttgart, Germany

²permanent address:
The Academy of Finland, P.O. Box 57, Fin-00551 Helsinki, Finland

³Motoren- und Turbinen-Union München (MTU), P.O. Box 50 06 40,
D-80976 München, Germany

⁴Agema Infrared Systems GmbH, Siemensstr. 20, D-64289 Darmstadt,
Germany

INTRODUCTION

The basic idea of nondestructive testing is that a sample is characterised by its response to a certain kind of excitation. The excitation may be an electric or elastic field with a time pattern described by a step, a pulse, or a sine wave type. The field can be applied locally to characterise the area around a certain sample spot. A raster scan image is then performed by measuring many spots one after the other.

That was the typical situation for thermal wave imaging derived originally from photo-acoustic spectroscopy where one observes the thermal response to a modulated optical input [1, 2]. Though this technique was soon extended to imaging [3, 4] there were serious restrictions to the size of the sample. Photothermal detection [5] removed this problem, however, it became clear that the depth range needed for many applications required such low modulation frequencies that it took a long time to generate an image. To give an example, to look 0.1 mm deep into polymers one needs about 1 Hz [6] even with signal phase [7-9]. This may be acceptable for a point measurement, but not for one pixel of an image. The only way to avoid a long image generation time at low modulation frequencies is to use a multiplex technique where all pixels are dealt with in parallel. This

can be achieved by generating and monitoring the thermal wave everywhere in the sample at the same time. So one can use a lamp to illuminate the whole sample periodically and a thermography camera to observe the resulting temperature modulation [10-12]. Phase and magnitude at each pixel are calculated in the simplest way from four thermographic images taken during one modulation cycle so that there is a constant phase angle of 90 degrees between subsequent images. If these are denoted by S_1 to S_4 , then phase φ and magnitude A are given by [12]

$$\varphi = \arctan \frac{S_3 - S_1}{S_4 - S_2} \quad (1)$$

$$A = \sqrt{(S_3 - S_1)^2 + (S_4 - S_2)^2} \quad (2)$$

Due to the speed of modern thermography cameras, many images may be recorded during one modulation cycle at low frequencies. However, for sinusoidal modulation one can apply suitable averaging techniques ending up again in the four raw images given above which are particularly easy and fast to evaluate.

From the structure of equ. (1) it is obvious that this kind of modulation thermography provides a phase angle image which is not affected by local variations of thermal wave excitation (e.g. due to inhomogeneous illumination or optical structure of the surface [13]), infrared emission coefficient, or local change of average temperature [12]. So it provides information on thermal structures to a depth given by about twice the thermal diffusion length which can be adjusted via the modulation frequency. That is why multiplex photothermal imaging or lock-in-thermography is relevant for applications.

As the multiplex method is advantageous at low frequencies one can use various kinds of thermal wave generation which will be demonstrated in the following together with applications where near-surface inspection is of interest, e.g. coated or layered materials.

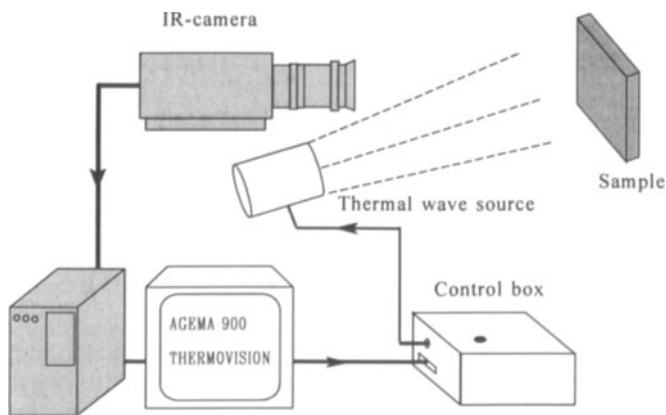


Fig. 1 Experimental arrangement for lock-in-thermography.

The arrangement for lockin-thermography is shown in Fig. 1 where a commercial thermography system (AGEMA 900) is coherently coupled to a thermal wave source which is operated in such a way that a sinusoidal temperature modulation results. This is achieved by automatically evaluating the thermographic data and by using a self-learning program which controls the power supply. After several modulation cycles to establish a stationary situation [14] the data acquisition starts. Time for measurements is typically below 2 minutes for frequencies between 1 Hz and 0.03 Hz.

The phase angle image displays basically the time shift between the remote heat injection and the remotely observed thermal response in the stationary oscillation. The thermographic image is the arithmetic average of the raw images S_1 to S_4 .

The thermal wave source can be a laser, a lamp (equipped with suitable filters to avoid cross-talk between excitation and detection), a beam of heated or cooled air (e.g. hot air gun), or even a combination of some of these sources. While these excitations are outside the sample (as drawn in Fig. 1), one can also think about selectively activating heat sources within the sample. Examples for this kind are resistive heating or mechanical loss-angle heating which results in a dark-field method.

EXAMPLES

The following examples have been selected to illustrate some fields of application and how the kind of excitation may be adjusted to the specific sample under inspection.

Coatings

Paint on polymer surfaces is still a real challenge for nondestructive testing since all methods fail which work so well for paint on metal because they are based on capacitive or inductive effects. Fig. 2 is an example showing how paint thickness variations appear in the phase angle image of lockin-thermography. Depending on the grey-level of the paint one may use a lamp or a hot air gun as a source. The method is also applicable to monitor thickness variations of ceramic coatings on metal substrates in a remote way, if the modulation frequency is low enough (Fig. 3).

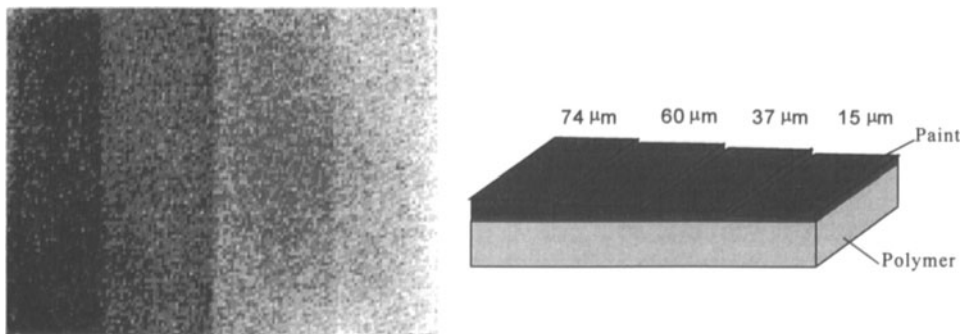


Fig. 2 Variation of paint thickness on polymer substrate monitored with phase angle image of lockin-thermography at the modulation frequency 0.93 Hz.

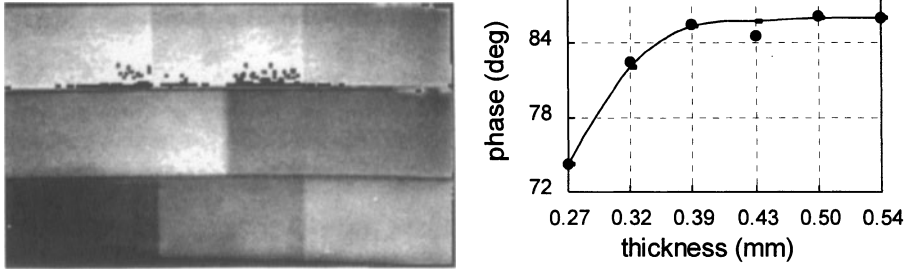


Fig. 3 Thickness variations of ceramic coating on metal substrate monitored with phase angle image at 0.06 Hz modulation frequency.

Such measurements are of relevance for the inspection of turbine blades where the ceramic coating provides protection against the heat. An additional heat protection is the internal cooling with flow through the subsurface channels of the blades.

Inspection of Subsurface Features

The sensitivity of the signal to thickness variations is the base for the inspection of internal structures, e.g. the very complicated cooling channels in turbine blades. Fig. 4a is a phase image obtained with a modulated hot air gun at 0.47 Hz. The light areas display the subsurface holes. On the lower right side the structures become less visible since their distance to the surface is larger. For comparison, Fig. 4b shows a result obtained on the same sample with pulse thermography. In that case the metallic surface of the turbine blade had to be painted black to improve the optical absorption for the flash lamp. Structures in the lower right side cannot be seen since they are out of range for most of the modulation frequencies in the continuous spectrum of the optical pulse.

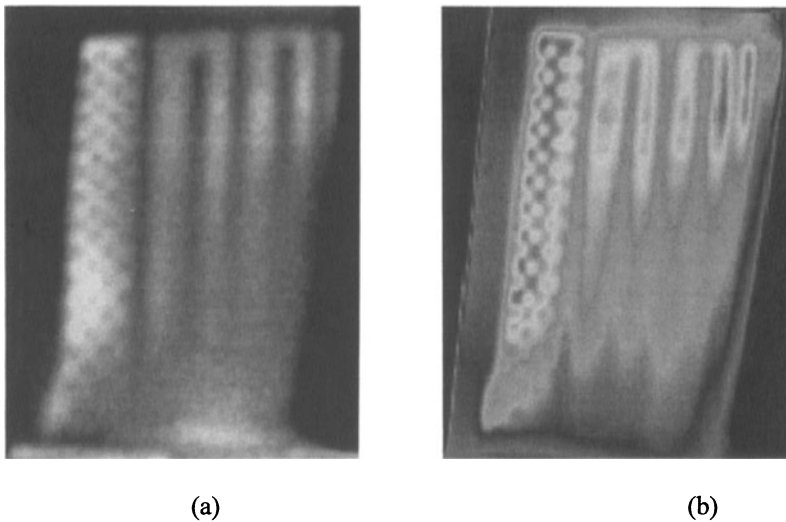


Fig. 4 Inspection of internal turbine blade structure, a) phase image of lockin-thermography at 0.47 Hz, b) result of pulse thermography (flash lamp) on same sample.

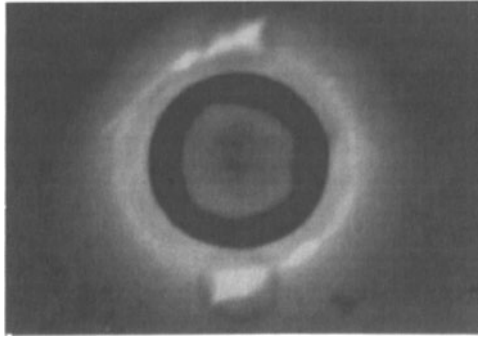


Fig. 5 Phase angle image of lockin-thermography taken at 0.06 Hz.

Carbon Fibre Reinforced Polymers (CFRP)

CFRP materials are important for lightweight structures due to their high specific strength. As these structures are often used in the safety relevant field of aircrafts and space vehicles, early detection of deterioration or generally of defects is of considerable interest, e.g. delamination or impact damage which may result in dangerous stress concentrations. Also in this case the defects are found by their influence on the boundary situation which affects modulated heat propagation. Fig. 5 is an example showing a repair pad with damage caused by cyclic mechanical loading. To investigate how well lockin-thermography competes with ultrasonic C-scan (requiring a liquid coupling agent) we performed comparative measurements on a CFRP sample provided with a hole where the area around the hole was delaminated due to a bending fatigue test (Fig. 6).

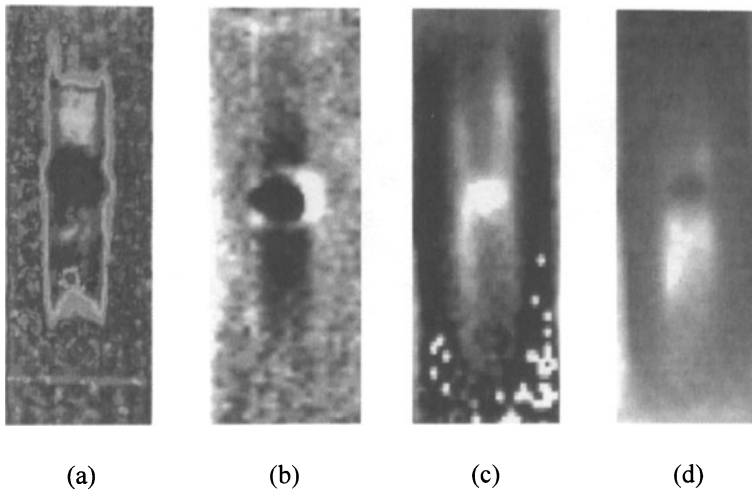


Fig. 6 Inspection of delamination caused by fatigue around a hole in a CFRP plate: ultrasonic C-scan (a), phase of lockin-thermography at 0.12 Hz (b) and phase (c) and magnitude (d) of lockin-vibrothermography using ultrasound of 40 KHz whose amplitude is modulated at 0.03 Hz.

As CFRP is electrically conducting one could also consider resistive heating [15]. Instead of these electrical losses we tried to use the mechanical loss angle for heating. Thermal effects due to mechanical loading are known from the SPATE-system based on the thermoelastic effect [16] and from vibrothermography [17] where the average temperature increase is used for imaging. In polymers the hysteresis effect is stronger than in metals. As the energy converted to heat depends on the hysteresis area (which is proportional to about the square of stress amplitude), the rate of heat generation depends approximately on the product of frequency and the second power of stress. High frequencies therefore allow to reduce the stress amplitude.

We extended this idea to amplitude modulated ultrasound: The carrier frequency of 40 KHz drives the heat generating hysteresis loop, the low modulation frequency generates the thermal wave. For ultrasonic coupling one edge of the sample was simply immersed into an ultrasonic cleaner. The result is shown in Fig. 6 (c) and (d). The delamination is clearly revealed both with phase and magnitude. The images look different since the magnitude image depends on how much elastic energy is converted to heat while the phase image shows the propagation time of the modulation to the surface.

Electronics

Heating with the electric loss angle (resistive heating) is attractive for electronic components which have built-in electrodes. Also in these cases the self-learning program applies a voltage resulting in a sinusoidal temperature modulation [18]. Fig. 7 displays images obtained on a resistor. The thermographic image (Fig. 7a) shows that the average temperature is about the same across the sample. The central vertical line is caused by superposed unmodulated reflection, the horizontal line in the upper part is the optical code point (silver ring) indicating the resistor quality. So all structure visible in the thermographic image is irrelevant or misleading.

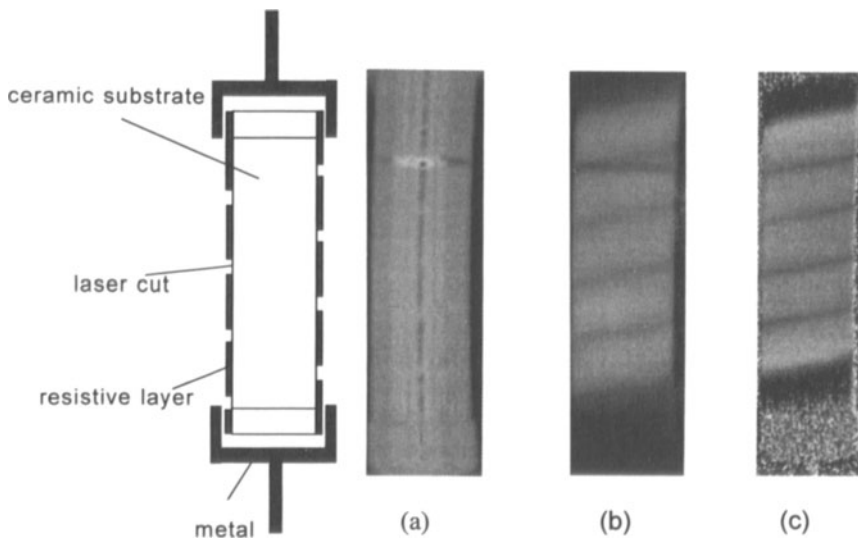


Fig. 7 Resistor inspected with thermography (a) as well as with magnitude (b) and phase (c) of lockin-thermography with current modulation at 0.23 Hz.

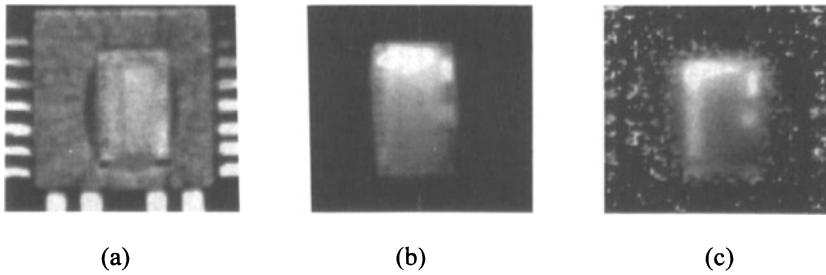


Fig. 8 Inspection of integrated circuit with thermography a) as well as magnitude b) and phase c) of lockin thermography with current modulation at 1.87 Hz.

In the amplitude image (Fig. 7b) the unmodulated reflection is eliminated, the optical ring is still visible. But this image already shows the localisation of temperature modulation. In the phase image (Fig. 7c) also the optical structure has disappeared, the darker areas indicate regions with some distance to the heating area. Phase angle lockin-thermography reveals which parts of electronic components are active while thermography displays only the overall average temperature.

Lockin-thermography with resistive heating is also informative if the object under inspection is more complicated. As an example Fig. 8 displays an integrated circuit where the supply voltage was modulated at 1.87 Hz. The thermographic image (Fig. 8a) shows all details since the whole sample including the substrate becomes warm. Both the magnitude (Fig. 8b) and the phase (Fig. 8c) of lockin-thermography show only the active part. Similar measurements have been performed on circuits imbedded in a chip, though at much lower resolution [19]. However such an image would also display areas where heat transport from the circuit to the surface suffers from additional boundaries.

CONCLUSION

Though the idea is not new that a sample can be characterised by its response to modulated heat deposition [20], the recent importance of lockin-thermography based on this principle has various roots

- modern thermographic systems perform fast and remote mapping of temperature fields
- computer controlled sinusoidal modulation and data analysis allow for fast evaluation of thermal wave data
- phase angle images do not contain misleading information
- thermal waves respond to subsurface boundaries with a depth range given by the modulation frequency. Thereby thermal wave tomography is possible on layered and coated materials.

Pulsed thermography with flash lamp excitation is an equivalent method in terms of mathematical evaluation. However, a pulse contains a broad spectrum where most of the power distribution is at modulation frequencies which do not fit to the required depth range. In these cases the thermal load is unnecessarily high which may be dangerous for organic or other sensitive materials.

ACKNOWLEDGEMENTS

We gratefully acknowledge partial funding of our research by BMBF project 03N8006BO. The samples used for Fig. 3 and Fig. 5 have kindly been provided by the Institute of Advanced Materials, Joint Research Centre of European Commission, Ispra (Italy) and Industrieanlagen-Betriebsgesellschaft mbH (IABG), Ottobrunn respectively.

REFERENCES

1. Y.-H. Pao (ed.) *Optoacoustic Spectroscopy and Detection* (Academic Press, New York, 1977)
2. A. Rosencwaig, *Photoacoustics and photoacoustic spectroscopy* (John Wiley & Sons, New York, 1980)
3. Y.H. Wong, R.L. Thomas, G.F. Hawkins, *Appl. Phys. Lett* 32, 538 (1978)
4. G. Busse, A. Ograbek, *J. Appl. Phys.* 51, 3576 (1980)
5. P.-E. Nordal, S.O. Kanstad, *Appl. Phys. Lett.* 38, 486 (1981)
6. A. Rosencwaig, A. Gersho, *J. Appl. Phys.* 47, 64 (1976)
7. G. Busse, *Appl. Phys. Lett* 35, 759 (1979)
8. R.L. Thomas, J.J. Pouch, Y.H. Wong, L.D. Favro, P.K. Kuo, A. Rosencwaig, *J. Appl. Phys.* 51, 1152 (1980)
9. A. Lehto, J. Jaarinen, T. Tiusanen, M. Jokinen, M. Luukkala, *Electr. Lett* 17, 364 (1981)
10. J.L. Beaudoin, E. Merienne, R. Danjoux, M. Egee, *Infrared Technology and Applications*, SPIE vol. 590, 287 (1985)
11. P.K. Kuo, Z.J. Feng, T. Ahmed, L.D. Favro, R.L. Thomas, J. Hartikainen, *Photoacoustic and Photothermal Phenomena*, (Hess P. and Pelzl J., Eds.) 415 (1988) Springer-Verlag, Berlin
12. G. Busse, D. Wu, W. Karpen, *J. Appl. Phys.* 71 8, 3962 (1992)
13. A. Rosencwaig, G. Busse, *Appl. Phys. Lett* 36, 725 (1980)
14. B. Rief, *Can. J. Phys.* Vol 64, 1303 (1986)
15. B. Rief, *Zerstörungsfreie Charakterisierung von kohlenstoff-faserverstärkten Kunststoffen mittels Wärmewellenanalyse*, University Stuttgart, Fakultät 13, Dissertation, VDI Düsseldorf (1988)
16. Patent No. PCT/GB 79/00081 and DE 2952809 C2
17. E.G. Henneke, K.L. Reifsnider, W.W. Stinchcomb, *Journal of Metals*, 11 (Sept. 79)
18. D. Wu, W. Karpen, K. Haupt, H.-G. Walther, G. Busse, *Journal de Physique IV*, C7, 567 (1994)
19. D. Wu, U. Palmer, G. Busse, *Inspection of electronics with lockin thermography*. Paper presented at conference QIRT '94 in Sorrento, Italy (Aug. 94)
20. M.A.J. Angström, *Phil. Mag.* 25, 130 (1863)